Journal Name

ARTICLE

Polymorphic transformation towards formation of nanotubes by self-assembly of an achiral molecule

Shuai Wang, Yajun Zhang, Yijun Xia, Bo Song*

In this paper, nanotubes with uniform diameter were prepared by self-assembly of an achiral azobenzene-containing fatty acid. The polymorphic transformation of the assemblies during the cooling process was systematically studied. By controlling the incubation temperature, different morphologies, such as membrane, stripes, helical ribbons and tubes, were all obtained in our experiment. These elements were all predicted by Selinger et al. in the theoretical model of the formation of nanotubes. To the best of our knowledge, this is the first experimental example to fully support their theory.

Introduction

Compared with the top-down technology, the bottom-up molecular self-assembly has provided us with a powerful, efficient, and convenient method to generate nanoscale artifacts with various morphologies and functions.[1-8] In recent years, self-assembly of amphiphiles has drawn a great deal of research attention and been utilized in a large variety of useful nanostructures with dimensions from zero to three.[9-16] As one case in point, the lipid nanotubes (formed in the dispersing mediums by self-assembly of different lipids, such as glycolipids, phospholipids, and peptide lipids) have been widely studied as a result of their high aspect ratio and hollow cylindrical morphology.[17-24]

Lipid nanotubes have advantages in terms of the one-step formation process without templates, the well-defined diameter, tunable surface property and flexibility.[18, 25-26] The unique properties allow lipid nanotubes potentials in encapsulation and release,[27-28] template synthesis,[29-31] catalysis,[32-33] and some specific usages in micro fluidic networks,[34] in molecular recognition devices,[35] and as liquid-crystalline biomaterials.[36-37] Despite the continuing emergence of new applications, fundamentals, such as the relationship between the nature of molecules and the morphologies of the resulting assemblies, are still the missing piece of the puzzle.[38] Fully understanding the mechanism of the formation of nanotubes is crucial to interpreting the various phenomena and suggesting the designs of lipid molecule.[19, 39]

Among the theoretical models used to describe the formation of lipid nanotubes, the elastic theory proposed by Helfrich and

Prost in 1988 has a far-reaching influence on the explanation of morphologies of nanotubes.[39] This theory claims that the tilt and chirality of the lipid molecules are essential to the intrinsic bending of the membrane, which results in the formation of tubular structure.[40]
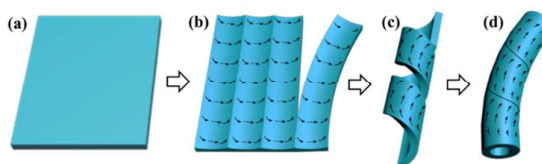
Scheme 1 The kinetic evolution from membrane to tube adapted from model proposed by Selinger et al.: (a) membrane, (b) stripe, (c) helical ribbon and (d) tube.

Helfrich's theory is widely accepted as the "uniform tilt" model, where the tilt direction is aligned in a uniform helical manner.[19] As an upgrade of the "uniform tilt" model, the "tilt modulation" model was proposed by Selinger et al.[21, 41] The latter emphasizes that the tilt direction varies across a membrane sheet, as shown in Scheme 1.[42-43] And the "tilt modulation" can only extend over a certain distance. The sharp domain walls will appear as the "tilt modulation" changes abruptly. The stripped walls break up and form a series of narrow ribbons during the cooling process of the dispersing mediums. These ribbons spontaneously twist into helices, which are intermediate species and eventually transform into tubular structures, as shown in Scheme 1c,d.

In the proceeding publications, some results have shown the morphic transformation from twisted/helical ribbons to tubular structures. For instance, Mezzenga et al. reported the time-resolved polymorphic states of assemblies of heptapeptide, and observed the formation of the three species in time order.[44] Analogous results expressed by different molecules were published separately by different groups, such as Stevens',[45] Lynn's,[46] Danino's[47] and Raphavan's.[48] It is worth

to note that Sharon et al. built a geometric-mechanical model for calculating equilibrium configurations of the self-assembled chiral ribbons, and used to quantitatively predict the twist-to-helical transition.[49] These publications serve as the experimental basis for the afore-mentioned theoretical models. Herein two points are necessary to be underlined. For one thing, the chiral center(s) was involved in most of the cases, but it is not a necessary condition for the construction of tubular structures. The examples without chiral center in the building blocks are the minority, but they are valuable supplementary to the theory proposed by Selinger et al. For the other thing, none of the publications up to date has shown all the morphological elements, such as membrane, stripes, helical ribbons, and tubes, in one self-assembly system. Such kind of demonstration would supply a full proof to the theory.

In this work, the self-assembly of an achiral azobenzene-containing long-chain fatty acid was systematically studied. A surprising result is that all the elements predicted in the theoretical model were all observed in the same system. The assemblies undergo polymorphic change with the alteration of temperature. This study provides experimental support to the theory proposed by Selinger et al.

Results and discussion

In this work, an azobenzene-containing long-chain fatty acid was designed and synthesized. The target compound is 4-(4-undecylazobenzene)butanoic acid, denoted by ABA11 for convenience of description. The synthetic route of ABA11 is shown in Scheme 2 (see the details in the experimental section). It is worth to note that, though column-chromatography has been run for several times, a small portion of molecules with cis-configuration steadily exists (NMR spectra in Fig. S1) in the final compound. That is, the original state of ABA11 used in this work is actually always a mixture of *trans-* and *cis*-configuration.
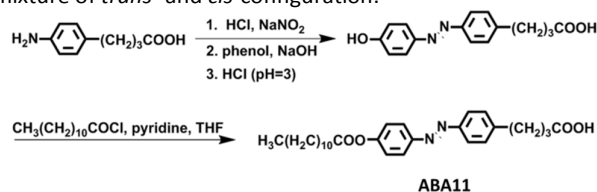
Scheme 2 The synthetic route of the target molecule ABA11.

As shown by the molecular structure in Scheme 2, ABA11 has no chiral center, and is namely an achiral molecule. While the azobenzene group will act as a kink or bend in the self-assembled structures, and has important consequences for generating a chiral packing.[50-52] If such kind of molecule can also undergo similar morphic transition like the molecules with chiral center, the result would be very interesting and serve as expansion to the theory proposed by Selinger et al.

DMSO is a selective solvent for ABA11, in which self-assembly will happen. A critical aggregation concentration (CAC) of 4.4×10^{-4} mol L^{-1} was determined by plot of turbidity against concentration (Fig. S2). The assemblies only formed when the

concentration is higher than the CAC (Fig. S3). During the self-assembly process, the solutions with different concentrations were kept at 80 °C for 0.5 h, and then slowly cooled to room temperature. And the self-assembly took a rather long duration to reach equilibrium. Typically, we observed the assembled structures after the solution was kept still for 2 months. As shown by the transmission electron microscopy (TEM) and atomic force microscopy (AFM) images in Fig. 1, nanotubes with high aspect ratio were obtained. The length of the nanotubes can reach to several micrometers. The TEM and AFM images show the consistent morphology and scale of the self-assembled structures. The diameters of the nanotubes were quite uniform. The values were approximately 36 and 38 nm determined by TEM and AFM, respectively. The slightly bigger diameter measured in AFM image is very possibly caused by the tip-enlargement effect. Therefore, the diameter indicated by TEM should be relatively more reliable. The thickness of the wall of the nanotubes (Fig. 1b) was approximately 6 nm. The extended length of ABA11 estimated by Chemdraw is 2.9 nm. Hence the wall of the nanotubes is about two times of the full length of the molecule, implying that the wall is composed of bilayer of ABA11. This result is further confirmed by the X-ray diffraction (XRD) and Fourier transform infrared spectroscopy (FTIR).
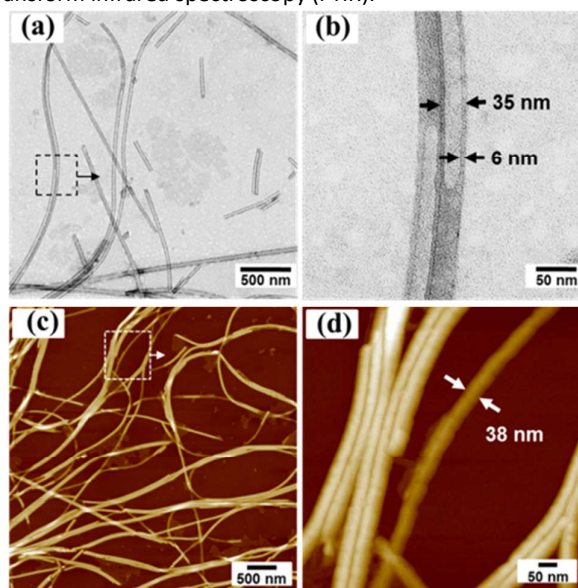
Fig. 1 (a) (b) TEM and (c) (d) AFM images of the nanotubes formed by ABA11 in DMSO solution. The solution (2×10^{-3} mol L^{-1}) was kept still at ambient conditions for at least 2 months.

The DMSO solution with assembled nanostructures was casted on glass substrate, and the film was characterized with XRD after the solvent was dried. As shown in Fig. 2a, the diffraction pattern shows periodic peaks at 7.67°, 10.72°, 12.24° and 13.80°. The corresponding d-spacings, calculated according to Bragg's equation, were 1.15, 0.83, 0.72 and 0.64 nm; the ratio of 1/5 : 1/7 : 1/8 : 1/9 is consistent with a membrane structure. The d-spacing of (001) plane can be extrapolated to

Nanoscale Accepted Manuscript

be 5.8 nm. This value matches well the thickness of the wall of the nanotubes determined by TEM images.
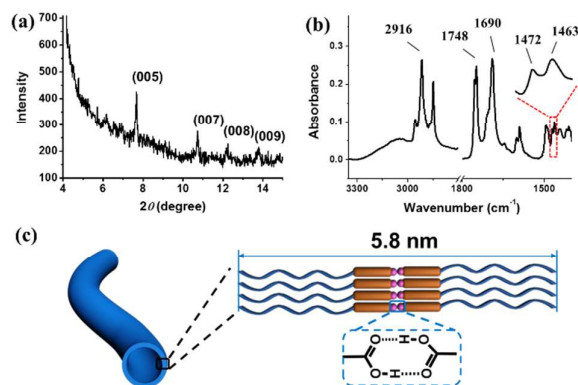
Fig. 2 (a) X-ray diffraction patterns and (b) FTIR spectra of nanotubes formed by ABA11, and the inset is the magnified part of the spectrum. (c) Schematic illustration of the packing of molecules in the wall of nanotube.

In addition to XRD, FTIR supplies more information about the interaction and packing of the molecules. As shown in the FTIR spectra in Fig. 2b, the vibration peaks located at 1748 and 1690 cm^{-1} are assigned to v(C=O) in ester bond and the terminal carboxylic groups, respectively. The rather low frequency of the latter suggests the formation of strong hydrogen bonding between carboxylic groups. And presumably, the ABA11 molecules were bonded together in form of dimmers. This makes a reasonable explanation for the TEM and XRD data. Other than the v(C=O), vibration peaks of CH$_2$ also provide useful information regarding to the molecular packing. The vibrational absorption of CH$_2$ antisymmetric stretching mode usually resides at 2925 cm^{-1}, while herein it shifted to 2916 cm^{-1}, suggesting the all-trans conformation of alkyl chains. Moreover, a splitting of the CH$_2$ scissoring band into 1472 and 1463 cm^{-1} can be assigned to an orthorhombic perpendicular subcell structure.[53] This result implies that the molecules are closely and orderly packed in the assemblies as shown in Fig 3c.
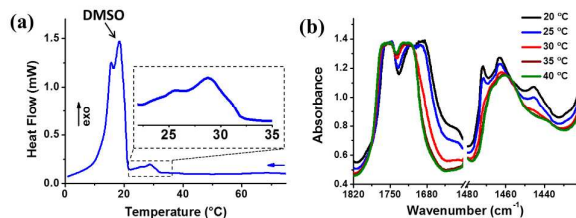
Fig. 3 (a) DSC of solution of ABA11 (scan rate 5 °C min^{-1}); (b) FTIR spectra of ABA11 in DMSO-d$_6$ collected at the temperature varied from 20 °C to 40 °C.

Temperature is one of the key factors that can affect the assembly dynamics.[54-57] As afore-mentioned, to fabricate the nanotubes, the solution was kept at 80 °C for 0.5 h, then cooled to ambient temperature. Very interestingly, we also noticed that when the temperature was halted for some time during the cooling process, different nanostructures were obtained. In order to figure out the possible phase transition

on cooling process, the differential scanning calorimetry (DSC) and temperature dependent FTIR were carried out.

Fig. 3a shows the cooling thermogram of ABA11 in DMSO. The peaks located at around 20 °C correspond to the exothermic peaks of DMSO, while the peaks centered at 25.5 °C and 29 °C should be assigned to the thermo-responses of ABA11. Since the thermogram analysis was conducted in DMSO, the transition points very possibly stand for the phase transition of the assemblies pre-formed in the solution. According to the literature, the peak centered at 29 °C may correspond to the phase transition of the alkyl chains, from a chaos state to an ordered arrangement.

This transition can also be supported by FTIR spectra. In doing so, deuterated DMSO was employed as the solvent to avoid the overlap of the vibrational signals. Spectra of ABA11 in DMSO-d$_6$ were measured from 20 to 40 °C with temperature intervals of 5 °C. On one hand, the regions corresponding to the vibration of carbonyl stretching were displayed in the left part of Fig. 3b. As the temperature was elevated to 30 °C, the absorption at around 1690 cm^{-1} shows a dramatic decrease in intensity, and the peak center shifted to higher wavenumber 1712 cm^{-1}. The contour of the curve keep unchanged as the temperature over 40 °C. The peak shift implies the variation of the hydrogen bonding between the carboxylic acid. On the other hand, the two peaks of CH$_2$ scissoring band merged into one broad peak upon heating, indicating a packing transition of alkyl chain from a highly crystalized state to chaos. Therefore, combining with the DSC result, it can be concluded that 29 °C corresponds to the interchange of the supramolecular interactions between the ABA11 molecules. We hypothesize that the change of the interactions should be correlated to the morphological transformation.
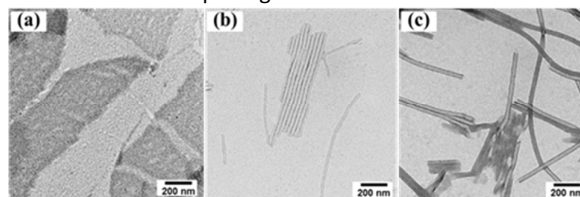
Fig. 4 TEM images of the assemblies formed by ABA11 at different incubation temperatures (a) 50 °C, (b) 35 °C and (c) 25 °C with the concentration of 5 × 10^{-4} mol L^{-1}.

In order to testify the hypothesis, the morphologies of the self-assembled aggregates of ABA11 were observed by TEM at different incubation temperatures, such as 50, 35, and 25 °C. The solution was heated to 80 °C, cooled to and kept at the set-points for 12 h, and then cooled down to 20 °C. The cooling process was controlled by low-temperature thermostat bath with speed of 5 °C min^{-1}. As shown in Fig. 4, three distinctive structures, flat membrane, stripes and nanotubes were observed at incubation temperature of 50, 35 and 25 °C, respectively. These structures are all mentioned in the model proposed by Selinger et al. At 50 °C, indicated by the merging of the CH$_2$ scissoring band in FTIR, the supramolecular interactions are relatively weak than that at 20 °C, and the mobility of alkyl chains is higher as well. Thus it is reasonable

that the anisotropic nature of ABA11 would result in the formation of membrane structures at these conditions. At 35 °C, which is close to the transition temperature, the supramolecular interactions were gradually coming into being, and the alkyl chains started to crystalize indicated by the tendency of splitting of the CH_2 scissoring band in FTIR. Under these circumstances, for one thing the molecules arranged more tightly and regularly, and for the other thing the carboxylic groups would adjust the posture to form hydrogen bonding. Combination of these two interactions explains the formation of the domains in the membrane, and the stripes in the matrix. At 25 °C, as the temperature is lower than the transition temperature, there is no surprise to see the nanotubes as that have observed at 20 °C. Nevertheless, it seems that some of the pieces for the puzzle were still missing, for example the transition state from membrane to stripes, and the process from ribbons to tubes. In the following, two experimental facts observed during the measurements compensated these two problems.

Fact 1

Fig. 5 shows the TEM and AFM images of self-assemblies of ABA11 formed at the incubation temperature of 40 °C. We happened to catch the on-going transition from membrane to ribbon-domains. As shown in Fig. 5a, part of the membrane has transferred to stripe-like structures. And the magnified image of Fig. 5a indicates the details of the transition. Most of the stripes were still sticking together, although the boundaries between them are very clear. Some of the ribbons have separated, and even peeled off from the matrix of the membrane. The TEM images are firm evidences for the transition from membrane to stripes. In addition, according to the section analysis of the AFM image (Fig. 5c,d), the average thicknesses of the fat membranes and the ribbon-domains were 6.1 and 4.2 nm, respectively. The thickness of the stripes is smaller than that of the membrane. This result accords with the theory proposed by Selinger et al. In the theory, Selinger et al. assume that the ribbons derive from the tilt modulation of molecules. That is to say, the shrink of the thickness is due to the tilt of molecules in the bilayer. Based on the above results and analysis, it can be concluded that the stripes stem from the phase transition of the alkyl chains and the tilt of the ABA11 molecules as the temperature decreases.

Fact 2

As depicted in Fig. 4, nanotubes were observed when the solution was prepared by incubating at 25 °C for 12 h and then quickly cooled down to 20 °C. Very interestingly, helical ribbons were also found in some regions. As shown in Fig. 6a, although most of the self-assembled structures were nanotubes, a special one with partial helical ribbon and partial straight ribbon was found. A schematic illustration was inserted in the TEM image. This structure serves as very good proof for the transition process of the self-assembled structures. It is quite accessible that the ribbons evolve into nanotube with the precursor of helical ribbons. The circular

dichroism (CD) signal shows a featureless line in the absorption region, indicating that the solution either contains no chiral elements or enantiomers. Combining with the images, our situation should belong to the latter. Generally, the molecular chirality is crucial and sometimes even decisive to the handedness of the assemblies. Although ABA11 has no chiral center, the self-assemblies of the molecule are chiral. It is reasonable that the rigid azobenzene groups can act as an asymmetric element of the molecule, which may give rise to the chiral stacking of ABA11.
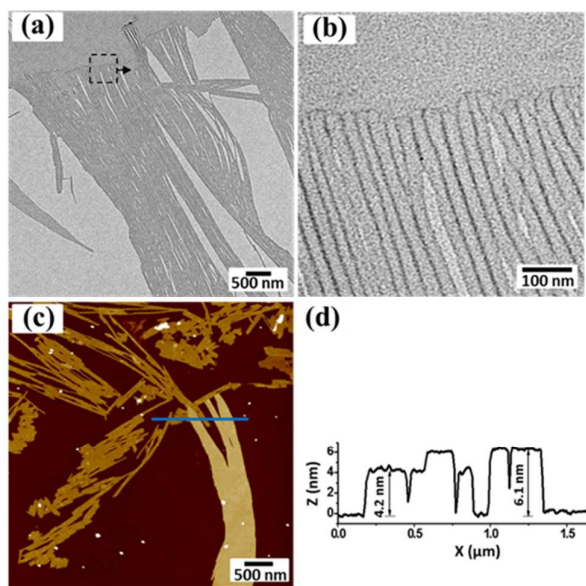
Fig. 5 (a) (b) TEM and (c) AFM images of the assemblies formed by ABA11 at the incubation temperature of 40 °C with the concentration of 5×10^{-4} mol L^{-1}. (d) is the section analysis of the AFM image.
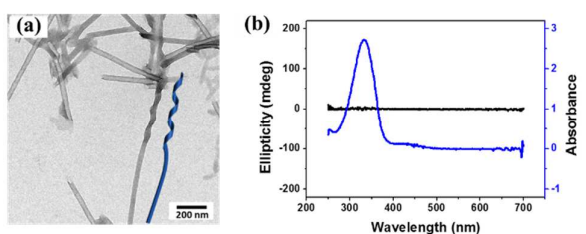
Fig. 6 (a) TEM images of the assemblies formed by ABA11 at the incubation temperature of 25 °C and (b) UV-vis and CD spectra of the aggregates (5×10^{-4} mol L^{-1}).

Till here, all the structures (such as membrane, stripes, helical ribbons and tubes) in the model proposed by Selinger et al. have been demonstrated in our experiment. And judging from the emerging sequence of the structures, the polymorphic transformation of the self-assembled structures is in good consistent with the theory.

As mentioned previously, the original state of ABA11 is always mixture of the two configurations. Thus, the influence of the configuration to the assemblies was investigated. As shown in Fig. 7a, after being irradiated for 10 min with 365 nm light, the peak at around 335 nm decreases dramatically, corresponding

to the conversion of the azobenzene group from *trans-* to *cis-*configuration. After irradiation, the nanotubes are no longer observed. The morphology of the assemblies, as shown in Fig. 7b, changed to spherical particles. These results indicate that the configuration is essential to the formation of the nanotubes. The reversibility of the morphological conversion in response to light irradiation was studied as well. Unfortunately, although the cis-configuration can be converted to trans-configuration upon irradiation, the spherical structures maintained.
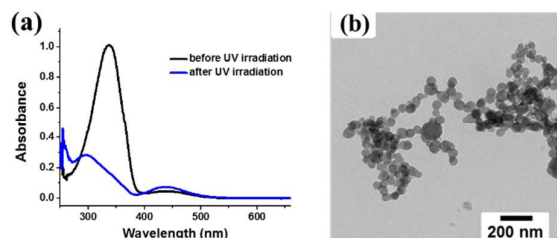
Fig. 7 (a) UV-vis spectra of ABA11 assemblies in DMSO before and after 10 min UV irradiation with 365 nm light. (b) TEM image of aggregates formed by ABA11 after UV irradiation.

Conclusion

We have synthesized an azobenzene-containing long-chain fatty acid ABA11 and found that this molecule can self-assemble into nanotubes with uniform diameter. The walls of nanotubes are composed of the bilayer of ABA11 molecules jointed by hydrogen bondings in between. By controlling the incubation temperature, all the structures, such as membrane, stripes, helical ribbons and tubes, which are proposed by Selinger et al., have been demonstrated in our experiment. More importantly, two key transition states in the formation of the self-assemblies were caught by chance. These results match well with the theoretical model and supply very good experimental support for it as well.

Experimental

Materials preparation

$NaNO_2$, NaOH, hydrochloric acid, phenol, THF, DMSO, ethyl acetate, petroleum ether and pyridine were purchased from Sinopharm Chemical Reagent Co., Ltd., and used as received. 4-(4-amino phenyl)butanoic acid was from Shanghai Boyle Chemical Co., Ltd.. Lauroyl chloride, $CDCl_3$, CD_3OD and DMSO-d_6 were bought from J & K Technology Co., Ltd.

Synthesis of 4-(4-((4-Hydroxyphenyl)diazenyl)phenyl) butanoic acid

The compound was synthesized according to a published procedure.[58]

Synthesis of 4-(4-((4-(dodec-1-en-2-ylperoxy)phenyl) diazenyl) phenyl)butanoic acid (ABA11 in Scheme 2)

To a 250 mL flask, under nitrogen protection and ice bath, 1.02 g (3.6 mmol) 4-(4-((4-Hydroxyphenyl) diazenyl)phenyl)butanoic acid, 15 mL THF and 3.2 mL (4 mmol) pyridine 1,6-diisocyanohexane were added. After being stirred for 15 minutes, 0.7 mL (3 mmol) Lauroyl chloride was added dropwise into the flask. The mixture was rose to room temperature and stirred for 24 h under nitrogen atmosphere. The reactant was filtrated and the solvent was removed under reduced pressure. The coarse product (dark-red solid) was dissolved in ethyl acetate, and washed with diluted hydrochloric acid (approximately 0.01 mol L^{-1}) for three times. The solvent was removed and the residue purified by aluminium oxide column chromatography (ethyl acetate: petroleum ether, 1 : 1) to give a light-yellow solid (0.43 g). Yield: 31%. ^{1}H NMR (400 MHz, $CDCl_3$): δ = 7.95 (d, J = 8.7 Hz, 2H; m-PhOOC), 7.85 (d, J = 8.0 Hz, 2H; o-azophenyl), 7.34 (d, J = 8.2 Hz, 2H; m-azophenyl), 7.24 (d, J = 8.7 Hz, 2H; o-PhOOC)，2.76 (t, J = 7.6 Hz, 2H; CH_2COOH)，2.59 (t, J = 7.5 Hz, 2H; CH_2COOPh), 2.41 (t, J = 7.4 Hz, 2H; $CH_2CH_2CH_2$COOH)，2.02 (m, 2H; CH_2CH_2COOH), 1.77 (m, 2H; CH_2CH_2COOPh), 1.43 (m, 2H; $CH_2CH_2CH_2$COOPh), 1.28 (m, 14H; $CH_3(CH_2)_7CH_2CH_2CH2$COOPh), 0.89 (m, 3H; $CH_3(CH_2)_{10}$COOPh).

Instruments

^{1}H NMR spectra for molecular structure characterization were recorded on a Bruker AVANCEIII 400 MHz (USA).

TEM characterization was performed using a Hitachi HT7700 (Japan) operating at 120 kV. The samples were casted to carbon-coated copper grids and measured without staining.

AFM images were recorded on a Multimode 8 microscope (Bruker, Santa Babara, USA). Peak force quantitative nano-mechanical mapping scan mode with ScanAsyst-Air probe (nominal spring constants 0.4 N m^{-1}, frequency 70 kHz, from Bruker) was adopted during the measurement.

XRD analysis of the nanotube was performed on a Brucker D2 Phaser X-ray diffractometer (Germany) with CuKa radiation (λ = 0.15406 nm) at 30 kV, 10 mA.

FTIR was measured using a Nicolet 6700 produced by Thermo Scientific (USA). The dry sample was prepared by casting the solution on the calcium fluoride (CaF_2) substrates, and then dried in vacuum. The liquid sample was prepared by loading about 10 μL of DMSO-d_6 solution of ABA11 in a liquid cell sandwiched between two CaF_2 slices, and the temperature dependent FTIR spectra were measured as the temperature was stable.

DSC characterization was carried out on the Mettler Toledo DSC1 (USA) calorimeter with the scan rate of 5 °C min^{-1}. The samples with different mass ratios of ABA11 were prepared by dissolving a certain amount of the solute into DMSO.

The incubation temperature was controlled by the low-temperature thermostat bath DC-2006 produced by Bilon (Shanghai) Instruments Co., Ltd. (China).

CD spectra were recorded on an AVIV 410 spectrometer (Aviv biomedical Inc).

The UV-vis spectra were obtained by using a UV-Vis spectrometer Cary 60 produced by Agilent Technologies (USA).

The UV light irradiation on the suspension of assemblies of ABA11 in DMSO was performed on a fibre lamp SP-9 equipped with a high-pressure UV source UXM-Q256BY produced by USHIO (Japan). The 365 nm light was irradiated on the samples for 10 min each time.

Acknowledgements

Notes and references

1   L. Zhang, X. Wang, T. Wang and M. Liu, *Small,* 2015, **11**, 1024.
2   Y. Qiao, Y. Lin, Y. Wang, Z. Yang, J. Liu, J. Zhou, Y. Yan and J. Huang, *Nano Lett.,* 2009, **9**, 4500.
3   A. H. Groschel and A. H. E. Muller, *Nanoscale,* 2015.
4   Y. Wang, P. Han, H. Xu, Z. Wang, X. Zhang and A. V. Kabanov, *Langmuir,* 2010, **26**, 709.
5   E. Busseron, Y. Ruff, E. Moulin and N. Giuseppone, *Nanoscale,* 2013, **5**, 7098.
6   X. P. Huang, Q. P. Qian and Y. P. Wang, *Small,* 2014, **10**, 1412.
7   L. Jiang, X. D. Chen, N. Lu and L. F. Chi, *Acc. Chem. Res.,* 2014, **47**, 3009.
8   L. Jiang, C. J. Zou, Z. H. Zhang, Y. H. Sun, Y. Y. Jiang, W. Leow, B. Liedberg, S. Z. Li and X. D. Chen, *Small,* 2014, **10**, 609.
9   C. Wang, Z. Wang and X. Zhang, *Acc. Chem. Res.,* 2012, **45**, 608.
10 T. G. Barclay, K. Constantopoulos and J. Matisons, *Chem. Rev.,* 2014, **114**, 10217.
11 G. M. Whitesides and B. Grzybowski, *Science,* 2002, **295**, 2418.
12 C. Wang, Z. Wang and X. Zhang, *Small,* 2011, **7**, 1379.
13 B. Song, B. Liu, Y. Jin, X. He, D. Tang, G. Wu and S. Yin, *Nanoscale,* 2015, **7**, 930.
14 Z. C. Shen, T. Y. Wang and M. H. Liu, *Chem. Commun.,* 2014, **50**, 2096.
15 Y. X. Tang, Y. Y. Zhang, J. Y. Deng, D. P. Qi, W. R. Leow, J. Q. Wei, S. Y. Yin, Z. L. Dong, R. Yazami, Z. Chen and X. D. Chen, *Angew. Chem. Int. Ed.,* 2014, **53**, 13488.
16 Y. G. Li, W. N. Wang, W. R. Leow, B. W. Zhu, F. B. Meng, L. Y. Zheng, J. Zhu and X. D. Chen, *Small,* 2014, **10**, 2776.
17 L. Zhang, C. Liu, Q. Jin, X. Zhu and M. Liu, *Soft Matter,* 2013, **9**, 7966.
18 N. Kameta, H. Minamikawa and M. Masuda, *Soft Matter,* 2011, **7**, 4539.
19 T. Shimizu, M. Masuda and H. Minamikawa, *Chem. Rev.,* 2005, **105**, 1401.
20 P. Bühlmann, L. Chen, J. Steed and P. Gale, Supramolecular Chemistry: From Molecules to Nanomaterials. Wiley New York: 2012.
21 O. Hayden and K. Nielsch, Molecular-and Nano-tubes. Springer Science & Business Media, New York, NY 10013, USA 2011.
22 W. F. Paxton, N. F. Bouxsein, I. M. Henderson, A. Gomez and G. D. Bachand, *Nanoscale,* 2015, **7**, 10998.
23 H. Xu, A. K. Das, M. Horie, M. S. Shaik, A. M. Smith, Y. Luo, X. Lu, R. Collins, S. Y. Liem, A. Song, P. L. A. Popelier, M. L. Turner, P. Xiao, I. A. Kinloch and R. V. Ulijn, *Nanoscale,* 2010, **2**, 960.
24 Z. Ren and P.-X. Gao, *Nanoscale,* 2014, **6**, 9366.
25 N. Kameta, K. Ishikawa, M. Masuda, M. Asakawa and T. Shimizu, *Chem. Mater.,* 2011, **24**, 209.
26 Y. Q. Liu, T. Y. Wang, Y. Huan, Z. B. Li, G. W. He and M. H. Liu, *Adv. Mater.,* 2013, **25**, 5875.
27 K. Ishikawa, N. Kameta, M. Aoyagi, M. Asakawa and T. Shimizu, *Adv. Funct. Mater.,* 2013, **23**, 1677.
28 K. Ishikawa, N. Kameta, M. Masuda, M. Asakawa and T. Shimizu, *Adv. Funct. Mater.,* 2014, **24**, 603.
29 C. N. R. Rao and A. Govindaraj, *Adv. Mater.,* 2009, **21**, 4208.
30 J. Zhang, G. Podoprygorina, V. Brusko, V. Böhmer and A. Janshoff, *Chem. Mater.,* 2005, **17**, 2290.
31 Y. Qiao, Y. Y. Lin, S. F. Zhang and J. B. Huang, *Chem. Eur. J.,* 2011, **17**, 5180.
32 S. Hudson, J. Cooney and E. Magner, *Angew. Chem. Int. Ed.,* 2008, **47**, 8582.
33 H. H. Yiu and P. A. Wright, *J. Mater. Chem.,* 2005, **15**, 3690.
34 N. Mahajan and J. Fang, *Langmuir,* 2005, **21**, 3153.
35 G. John, J. H. Jung, M. Masuda and T. Shimizu, *Langmuir,* 2004, **20**, 2060.
36 V. Vill and R. Hashim, *Curr. Opin. Colloid In.,* 2002, **7**, 395.
37 G. John, H. Minamikawa, M. Masuda and T. Shimizu, *Liq. Cryst.,* 2003, **30**, 747.
38 Y. Yan, Y. Lin, Y. Qiao and J. Huang, *Soft Matter,* 2011, **7**, 6385.
39 Z. Tu and Z. Ou-Yang, *Adv. Colloid Interface Sci.,* 2014, **208**, 66.
40 W. Helfrich and J. Prost, *Phys. Rev. A,* 1988, **38**, 3065.
41 J. Schnur, B. Ratna, J. Selinger, A. Singh, G. Jyothi and K. Easwaran, *Science,* 1994, **264**, 945.
42 J. V. Selinger, M. S. Spector and J. M. Schnur, *J. Phys. Chem. B,* 2001, **105**, 7157.
43 J. Selinger, F. MacKintosh and J. Schnur, *Phys. Rev.E,* 1996, **53**, 3804.
44 J. Adamcik, V. Castelletto, S. Bolisetty, I. W. Hamley and R. Mezzenga, *Angew. Chem. Int. Ed.,* 2011, **50**, 5495.
45 J. Song, Q. Cheng, S. Kopta and R. C. Stevens, *J. Am. Chem. Soc.,* 2001, **123**, 3205.
46 K. Lu, J. Jacob, P. Thiyagarajan, V. P. Conticello and D. G. Lynn, *J. Am. Chem. Soc.,* 2003, **125**, 6391.
47 L. Ziserman, H.-Y. Lee, S. R. Raghavan, A. Mor and D. Danino, *J. Am. Chem. Soc.,* 2011, **133**, 2511.
48 H. Y. Lee, H. Oh, J. H. Lee and S. R. Raghavan, *J. Am. Chem. Soc.,* 2012, **134**, 14375.
49 S. Armon, H. Aharoni, M. Moshe and E. Sharon, *Soft Matter,* 2014, **10**, 2733.
50 Y. Lin, Y. Qiao, P. Tang, Z. Li and J. Huang, *Soft Matter,* 2011, **7**, 2762.
51 Q. C. Hu, Y. Y. Wang, J. Jia, C. S. Wang, L. Feng, R. H. Dong, X. Sun and J. C. Hao, *Soft Matter,* 2012, **8**, 11492.
52 T. G. Barclay, K. Constantopoulos, W. Zhang, M. Fujiki, N. Petrovsky and J. G. Matisons, *Langmuir,* 2013, **29**, 10001.
53 N. Kameta, K. Ishikawa, M. Masuda and T. Shimizu, *Langmuir,* 2013, **29**, 13291.
54 H. Yui, H. Minamikawa, R. Danev, K. Nagayama, S. Kamiya and T. Shimizu, *Langmuir,* 2008, **24**, 709.
55 U. Bernchou, H. Midtiby, J. H. Ipsen and A. C. Simonsen, *BBA-Biomembranes,* 2011, **1808**, 2849.
56 A. L. Fameau, F. Cousin, L. Navailles, F. Nallet, F. Boue and J. P. Douliez, *J. Phys. Chem. B,* 2011, **115**, 9033.
57 R. O. Brito, I. S. Oliveira, M. J. Araujo and E. F. Marques, *J. Phys. Chem. B,* 2013, **117**, 9400.
58 S. Wang, N. Zhang, X. Ge, Y. Wan, X. Li, L. Yan, Y. Xia and B. Song, *Soft Matter,* 2014, **10**, 4833.